Performance of Real-Time Geospatial Spectrum Sharing (RGSS) between 5G Communication Networks and Earth Exploration Satellite Services

Elliot Eichen Choyu Networks Boston, MA USA elliot.eichen@choyu.net

Abstract—A proof of concept system that enables real-time geospatial spectrum sharing between 5G/6G networks and Earth Exploration Satellite Services (EESS) has been developed. A simple algorithm that pauses network transmissions when there is potential interference from 5G/6G transmitters provides 99.6% network availability in the 24 GHz NR2 band while protecting all currently working EESS radiometers operating in the 23.8 GHz band. A more sophisticated algorithm that modifies transmission power levels and (if necessary) network traffic (similar to the methodologies used by Citizens Broadband Radio Service) can reduce interference so that there is no adverse impact on network availability. In addition to preventing interference, RGSS provides other significant benefits to both the wireless and the weather/climate communities, including improving network performance and coverage, the ability to support changes in network architectures, network elements, endpoints, and new or more sensitive radiometers, and a simple mechanism to test and police compliance with out-of-band emission requirements. RGSS is also compatible with existing spectrum management systems.

Keywords—5G, 6G, mm-wave, out-of-band emissions, spectrum sharing, earth exploration satellite services, spectrum management.

I. INTRODUCTION

Increased demand for wireless services has created competition for RF spectrum between 5G/6G wireless communications and legacy applications such as remote sensing, GPS, and radar systems. This competition has encouraged the development of new methods for spectrum sharing that enable legacy applications to co-exist with wireless networks. One example of a geospatial sharing mechanism already deployed in the US is Citizens Broadband Radio Service (CBRS) [1], where mid-band (3.5 – 3.7 GHz) spectrum is shared between legacy spectrum users (Department of Defense radars, EESS communication downlinks, and some wide area network broadband protocols) and wireless service providers. Another proposal for geospatial-based sharing of mm and sub-mm wavelengths between wireless networks and EESS radiometers (used to gather data for weather forecasting and longer-term climate modeling) was presented at this conference in 2019 [2].

In this paper, a proof-of-concept (POC) system¹ – Real-Time Geospatial Spectrum Sharing (RGSS) – based on the 2019 proposal will be discussed. Using the issue of interference between 5G NR2 band transmitters (24.25 – 24.75 GHz) and EESS radiometers (23.7-23.9 GHz) [3,4] as a test case, a simple RGS algorithm that pauses communications while a base station

(gNB) is within a radiometer's measurement pixel provides a network availability of 99.6% for the aggregate of *all* satellite/radiometer operating in the 23.8 GHz band. A more sophisticated algorithm that models the interference using network infrastructure data plus specific radiometer characteristics and traversals has also been investigated. This algorithm works by reducing Tx power, and by moving network traffic (if required) to alternate bands using the 3GPP dual-active stack protocol [5] when and where interference will occur. Since interference is likely to be present only in dense urban environments (and therefore in a small number of pixels), network elements in suburban and rural areas can operate "hotter" than those in major cities, enabling increased coverage and better economics for carriers.

As a software solution, RGSS provides advantages to both the wireless and weather/climate communities. RGSS:

- Enables carriers to optimize network performance by geography, rather than requiring vendors to deliver base stations (gNBs) and user equipment (UEs) designed for worst-case interference scenarios. This optimized performance can be instrumental to providing service in suburban and rural deployments.
- Requires only one (software) system to support spectrum sharing across multiple mm-wave and sub-mm-wave bands (e.g., 24,52,90, and 130 GHz). Moreover, RGSS is consistent with the architecture and operations of Spectrum Management Systems (SMS) defined by the wireless innovation forum and is currently used to prevent interference in CBRS networks.
- Can quickly support changes in 5G/6G network architectures and new network elements or devices.
- Accommodates future radiometer sensors and satellites, and future changes to international standards for isolation between communication networks and radiometer measurements, and
- Provides a simple mechanism to test and police compliance compared with in-situ over the air Total Radiated Power (TRP) measurements.

been relabeled as Real-Time Geospatial Spectrum Sharing (RGSS) for clarity.

¹ The 2019 concept was titled Dynamic Geographical Spectrum Sharing. Based on input from various colleagues, this method has

II. CURRENT (ITU) METHODOLOGY TO PREVENT INTERFERENCE BETWEEN 5G NETWORKS AND EARTH EXPLORATION SATELLITE SERVICES

To understand how RGSS works, it is helpful to review how the International Telecommunications Union (ITU) defines and calculates the amount of interference between mobile networks and EEES radiometers. The ITU's recipe for calculating interference [6] relies on a Monte Carlo simulation of a 5G network, which in turn is based on many assumptions such as density of base stations (gNBs), antenna characteristics (heights, azimuth angles, gains, the number and pattern of MIMO arrays, far fields), coherence in adjacent spectrum, endpoint density and power levels, etc. It also requires many other inputs such as the geographical area over which to consider the number of interfered with pixels (figure 1), a specific reference radiometer, and ITU specifications for calculating atmospheric attenuation, clutter, network loading, UE (User Equipment) power control, etc.

To determine the emission limits necessary to prevent interference, the RF power from an International Mobile Telecommunications (IMT) network detected by a EESS radiometer is calculated as the sum of RF power from all mobile network antennas within a measurement time step (or pixel see next section) and within the electrical bandwidth of the reference radiometer. The total radiated power (TRP) from each IMT antenna is then scaled so that the IMT power at the radiometer from all antennas does not exceed the noise equivalent power (usually expressed as an equivalent noise temperature in ok) of the test radiometer for 99.99% of all time steps. For the case of the 24 GHz communications band (24.25-24.75 GHz), EESS radiometers operate in the adjacent 23.8 \pm 100 GHz band. The limit on RF from the IMT transmitters that leaks into the radiometer band is therefore called the out-ofband (OOB) emissions limit.

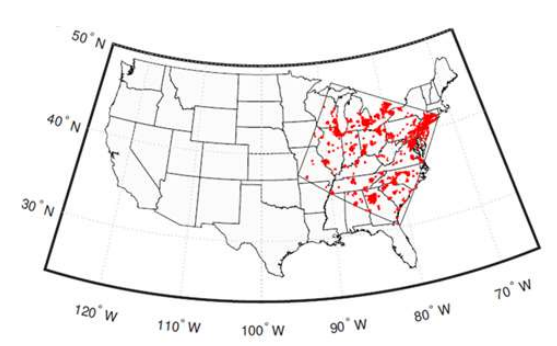


Figure 1: geographical area defined by IMT for calculating OOB emissions. From [7].

Several key points about the ITU methodology are:

 Once the ITU World Radio Congress (WRC) agrees on a specific OOB emission limit², network and UE vendors design, test, and certify their equipment to meet this limit. Emission limits are typically implemented in hardware

- based on carefully selected and engineered microwave components.
- 2. Emission limits are calculated for a reference (typically very sensitive) radiometer. A higher emission limit could be used to protect other less sensitive radiometers from interference, but since network and UE equipment does not distinguish between radiometers, network equipment cannot take advantage of these less sensitive radiometers.
- 3. Even for the sensitive reference radiometer used to calculate the OOB emissions limits, 99.99% of all pixels can tolerate higher emissions limits, resulting in reduced network performance for the vast majority of pixels (or geographical areas) subtended by any given radiometer traversal.
- 4. The process for setting emission limits is long, typically taking at least four years (the ITU regulatory cycle time). This creates risk for network and device vendors and/or limits the deployment of new network architectures. Moreover, managing interference by engineering IMT hardware increases interference risk if and when more sensitive radiometers become available.

III. RGSS: METHOD OF OPERATION

Conceptually, RGSS is similar to the ITU's recipe for calculating interference between IMT networks and EESS radiometers, except that RGSS uses existing (deployed) network infrastructure and actual satellite traversals and radiometer characteristics. This data is provided to a spectrum management system that models the RF environment and modifies Tx power and network traffic to meet OOB emission limits.

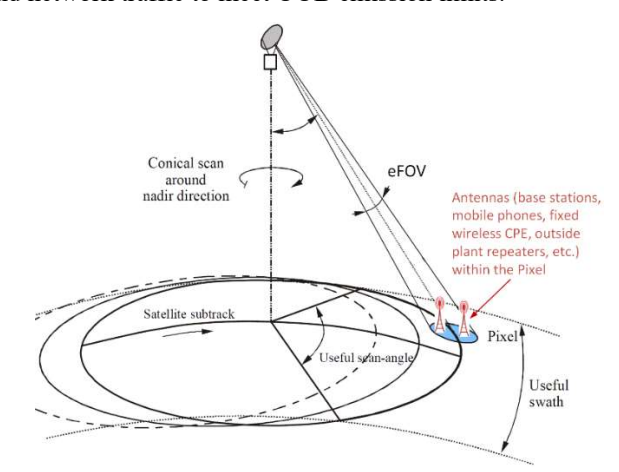


Figure 2 – Geometry of a conical scan radiometer. From [10]

From figure 2, a measurement pixel computed from the effective field of view (eFOV) of the radiometer (i.e., the projection of the radiometer's aperture in the sensor's object plane) is scanned across the Earth as its satellite moves in orbit. RF radiation produced by IMT transmission antennas within each pixel is captured by the radiometer along with the RF produced by atmospheric water vapor (and other molecular species) rotational states. Since radiometers measure power integrated over a relatively long time compared with the symbol time of the communications system, radiometers are unable to distinguish detected power due to IMT network transmissions

² And presumably the member nations ratify or accept this limit.

(the noise) from detected power due to atmospheric molecular rotational transitions (the signal). When the radiation from the sum of all IMT antennas reaches the noise equivalent power of the radiometer, the measured data becomes corrupted and results in incorrect weather predictions [8] or baseline data used for climate models [9].

A. Simple RGSS Algorithm

The most straightforward algorithm implemented by the RGSS POC is to pause transmissions from all IMT antennas within a given pixel. While simple, this algorithm results in unnecessarily pausing transmission in places where the RF from IMT antennas is small enough (due to gNB density, radiometer sensitivity, or distance/angle between the radiometer and pixel) such that interference would not have occurred. The advantage of the simple algorithm is that it does not require a propagation model to calculate interference and only requires gNB locations (rather than more detailed knowledge about the IMT's network infrastructure).

To find the average total pause time/day requires calculating the pixel areas for each measured pixel for each satellite/radiometer traversal, and then averaging the pause time over many days of traversals for all possible satellite/radiometers. This calculation takes into account the differences between cross-track, conical, and non-scanning (nadir only) radiometers, along with pixel size variation as a function of scan angle (for cross-track radiometers).

Table 1 shows the total average pause time all satellite/radiometers that measure radiation in the 23.8 GHz band. These calculations use TLE [11] satellite orbital data and operational status (Celestrack[12]), and radiometer parameters needed to calculate pixel size and scan rates (from WMO-OSCAR [13] and various technical papers [14-16]). Nonscanning (down-looking nadir only) radiometers need to be included in a production system for network pausing. However, it is unnecessary to add them in calculating the average daily pause time as they do not contribute in a meaningful way to diminishing availability (they typically provide full earth coverage over a month and have small pixel areas, compared with scanned radiometers that sample all portions of the Earth at least twice a day, and that typically have much larger pixels). One conical scanned radiometer - Madras, riding on Megha Tropiques – can also be left out of the average daily pause time as it is in a near-equatorial orbit rather than near-polar orbit and does not appear to traverse the continental US.

In addition to pausing transmission in the measurement pixel, it is necessary to pause transmission in a buffer around a measurement pixel to accommodate uncertainty in the calculated pixel position and size. In the case of cross-track scanners, the radiometer scanning period is synchronized with the satellite's position [17]. When using ATMS pixel position data for times 12 hours prior to a given transversal [18], RGSS could predict a radiometer's scan cycle accurately enough to such that the position of the calculated pixel to the actual pixel was \pm 5km. It was thus reasonable to use pixel-based geo-fencing to buffer the

pixel area for cross-track radiometers. RGSS uses a box of one pixel in width and height around each measured pixel to compute the pause time (Figure 3). Because of oversampling by ATMS, this buffer subtends 81 pixels (9x9 array)³.

			Pixel-	Line-	
			geofencing	geofencing	total pause
	radiometer	# active	[sec/day-	[sec/day-	time/day-rad
radiometer	type	satellites	satellite]	satellte]	[sec]
AMSR-E	conical	1		30.8	30.8
AMSU-A	crosstrack	6	4.2		25.2
ATMS	crosstrack	2	9.8		19.6
GMI	conical	1		5.25	5.25
MTVZA-GY	conical	3		128.6	128.6
MWRI (HY2)	conical	2		107.9	107.9
MWRI	conical	4		64.5	64.5
WindSat	conical	1		2.4	2.4
AMR	nadir				
MADRAS	conical equa	384.25			
MWR (Sentinal 3	network availability				99.6%
AMR-C	nadir				
Altika	nadir				

Table 1: Average pause time/day for all operational radiometers & satellites.

In contrast to cross-track radiometers, conical radiometers scan open-loop compared with the orbital motion of the satellite. It is therefore impossible to accurately predict where the radiometer will be in the scan cycle as a function of the radiometer position. In this case, RGSS uses a ± 1 scan line as a buffer for calculating pause times. This results in substantively longer pause times for conical radiometers compared to scanned radiometers.

Combining the pause times for all conical radiometer/satellite traversals with cross-track radiometer/satellite traversals, the total network availability time (1 - total pause time [seconds/day] ÷ total time [seconds/day]) is found to be 99.6%. While 99.6% is about the same as the outage time for CBRS across its entire area of operation, it is less than the network availability generally desired for a telecommunications service⁴. In terms of network isolation, pausing all transmissions from antennas within a radiometer's eFOV should reduce the interference to zero. In practice, this need to be confirmed by active physical layer testing using a test transmitter with adjustable zenith angle, azimuth angle, ERP, in conjunction with a near-polar orbit radiometer.



Figure 3 – pixel with saftey buffer (in blue).

³ By comparison, AMSU does not oversample. However, AMSU has a considerably longer cycle time (8sec) than ATMS (2.7sec).

⁴ However, CBRS dynamic protection areas (DPAs) tend to be greographically constrained to a small number of locations, while RGSS DPAs *for the simple algorithm* are uniformly distributed.

B. More Sophisticated RGSS Algorithm

While the simple RGSS Algorithm (A) is valid, a more sophisticated algorithm is required to obtain higher network availability. RGSS' more sophisticated algorithm calculates the detected RF power from the IMT network produced within the bandpass of a specific radiometer using actual network infrastructure data for all radiometer/satellite traversals. In addition, this algorithm takes advantage of time-of-day and day-of-the-week historical data⁵ to project likely network traffic. These traffic estimates can be added to shape the calculation of received IMT power.

To motivate this discussion, consider figure 4, which shows the pixel geometry/area for three different radiometers at different points in their scans. In the case of the two cross-track radiometers (ATMS and AMSU-A), the pixels become elliptical and significantly larger at the edge of their scans and smaller and circular when the radiometer is pointed straight down from the satellite (nadir). If antenna density is proportional to the pixel area (while this is unlikely to be rigorously correct – antenna placement is a complex process for carriers, dictated by many factors including geography, population density, frequency planning, the availability of antenna sites, etc. – it is reasonable as a rough order of magnitude approximation), then the reduction in OOB emission power @ 23.8 GHz for a radiometer compared to ATMS that takes into account the number of antennas within a pixel along with the sensitivity and bandwidth of the radiometer, is given by:

$$\begin{split} \Delta \, OOB \, [dB] \, = \, & 10 \log \left(\frac{NE\Delta T}{NE\Delta T_{ATMS}} \right) + \, \, 10 \log \left(\frac{\Delta f}{\Delta f_{ATMS}} \right) + \\ & 10 \log \left(\frac{PixArea}{PixArea_{ATMS}} \right) \end{split}$$

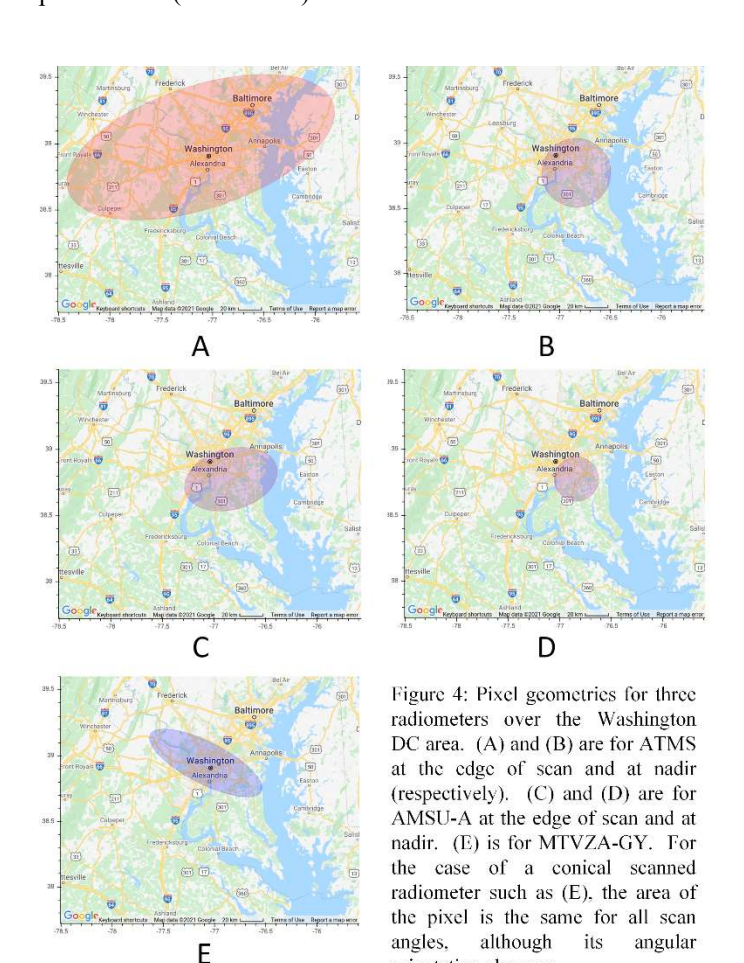
		noise equiv	radiometer	OOB emissions reduction compared with ATMS [dB]			Satellites
	[GHz}	ΔT	type	nadir	max	average	
ATMS	0.27	0.90	crosstrack	0	0	0	SUOMI NPP, NOAA 20
							NOAA 15, NOAA 18, NOAA
							19, METOP B, METOP C,
AMSU-A	0.27	0.30	crosstrack	9	11	9	Aqua
AMSR-2	0.40	0.60	conical	12	21	15	GCOM W
GMI	0.37	1.05	conical	13	23	17	GPM Core Observatory
AMSR-E	0.40	0.60	conical	13	22	16	Aqua
WindSat	0.50	0.55	conical	8	17	11	Coriolis
MWRI	0.40	0.50	conical	8	17	11	FY-3B, FY-3C, FY-3D, FY-3E,
MWRI(HY2)	0.40	0.50	conical	9	18	12	HY-2A, HY-2B
	0.40	•		,			Meteor-M 1, Meteor-M 2,
MTVZA-GY	0.40	0.30	conical	5	14	8	Meteor M2-2

Table 2: Change in OOB emissionS per radiometer & satellite traversal.

Table 2 shows the reduction in OOB emissions compared to ATMS for all active radiometer/satellite pairs. While these results should not be taken as being numerically accurate (because of the rough approximation of constant pixel density), the large difference in OOB emission power (as much as 17dB for the average pixel size and 23 dBi for pixels at their maximum scan angle) they show that dynamically accounting for RF interference on a per satellite traversal/radiometer and pixel basis can significantly increase range and coverage when

a less sensitive/smaller-pixel radiometer/satellite traversal is encountered. Similarly, they show that better isolation for interference can be obtained when the radiometer/satellite traversal of a sensitive radiometer with a large pixel size is encountered.

The metric for measuring the efficacy of the more sophisticated algorithm is the amount of traffic that needs to be moved to other bands when an antenna is within the measurement pixel. While it is not possible to accurately determine the % of pixels that would contribute enough RF power to interfere with radiometer measurements without actual 5G/6G network infrastructure data⁶, it is possible to develop processes to limit OOB emissions in pixels that would otherwise be corrupted. These processes include calculating and moving sufficient network traffic to other bands to bring the OOB emissions level below the acceptable limit or pausing some network traffic. Moving traffic (based on Class of Service) is preferable to pausing traffic not only for service continuity but because the handover time for 5G networks (less than a few msec to meet latency requirements) is considerably less than the UEs registration time. 3GPP introduced the Dual Active Protocol Stack handover mechanism in rel 16 [5] to provide fast (a few msec) handovers between bands.



 $^{^{5}}$ Insteand of historical data, real-time traffic data could be read from the IMT network.

orientation changes.

⁶ Or, with less accuracy, a full Monte Carlo simulation similar to the one used in [6].

IV. FUTURE-PROOFING

One advantage of a software solution such as RGSS compared to hardware-based methods for preventing interference is that new network elements or architectures, or radiometers with lower noise figures, can be quickly accommodated. This enables both communications AND weather/climate ecosystems to rapidly adopt new or improved technologies while avoiding interference. A more complex problem is how RGSS might cope if the number of traversals/day used by weather models were to increase, perhaps by flying small sat radiometer constellations. Since such constellations would presumably use lower-cost satellites and instruments, in this case it might be possible to divide frequency bands between satellites so that not all bands would be subject to RGSS control at the same time.

Two examples of where new technology has out-paced the existing regulatory and development environment for setting hardware-based interference limits are the deployment of outside plant 5G network repeaters [19] and the introduction of high power (3GPP class 1) customer premise equipment (CPE) for fixed wireless access (FWA)[20]. Network repeaters and high power FWA-CPE were not included in computations or discussions that led to OOB emission limits ratified at WRC-19. However, both of these device classes will increase the interference from OOB emissions. Network repeaters are currently being deployed in significant numbers inside of 5G cells, and thus they increase the density of transmitters. High power FWA-CPE (if exempt from regulatory limits on OOB emissions, as has been requested by CPE manufacturers [21]) can significantly increase OOB emissions because the TRP and ERP from these devices is much higher than the UEs considered by the ITU (handsets). Moreover, even if FWA-CPE does meet the ITU OOB emission limits, they may still significantly increase interference if they avoid implementing a power control algorithm [22] specified by 3GPP to limit battery drain. (And there is no need for FWA-CPE to implement the power control algorithm as these devices use line electric power).

By contrast with the present methodology, once outside plant repeaters and high power FWA-CPE were added to RGSS' network infrastructure schema (a few hours of work), they immediately became part of OOB emission calculations and thus integrated into interference mitigation actions.

Another aspect of software solutions such as RGSS is that their output can be easily audited. This provides a more straightforward path to verify and police compliance than making TRP measurements (particularly when those measurements need to be made in situ).

V. GEOPOLITICAL IMPLICATIONS

Communications network infrastructure is clearly a sensitive strategic defense issue for most nations. Moreover, weather forecasting and the ability to corrupt these forecasts can (in principle) be weaponized. Even though a full discussion of the geopolitical implications of RGSS is beyond the scope of this

paper, it is important to acknowledge that all geospatial models used to prevent interference have geopolitical implications.

While the development and distribution of RGSS does not require actual network infrastructure data, each actual implementation does. To mitigate the concerns related to leakage of sensitive data, we expect that systems such as RGSS would be hosted and run by entities inside each nation. We also expect that compliance would be verified by both performance auditing and by remote sensing capabilities. Alternatively, geospatial spectrum solutions could be implemented by some (rather than all) ITU members⁷. However, this would require network and UE vendors to support both hardware and software solutions.

VI. COMPARISON WITH CBRS

It is interesting to compare system architecture and network availability of an operational geospatial spectrum sharing system (CBRS) with RGSS. Citizens Band Radio Service, which began US operations in late 2020, shares 150 MHz of spectrum between 3.55-3.7 GHz with incumbent users: Department of Defense radars, EESS communication downlinks, legacy Part 90 broadband services, and radio-astronomy sites. CBRS uses a Spectrum Access System (SAS) defined by the Wireless Innovation Forum [23] to ensure that incumbent spectrum users are not interfered with within specific Dynamic Protection Areas (DPAs). The SAS models the RF environment and controls base station transmissions and power levels. While radio-astronomy sites and some military sites are permanently geofenced, other DPAs are dynamically geo-fenced using either environmental sensing (e.g., a sensor connected to the SAS detects use of the band by incumbent users, such as a Navy radar system in given DPA), or scheduling (e.g., the Navy has informed the SAS that it will be using spectrum in a given DPA on Friday from 11 AM through 5 PM).

	CBRS	RGSS	
deployment status	operational	proposed	
f	mid-band (3.55-3.7 MHz).	mm to sub-mm	
frequency band	Proposed use 6Ghz	(20 GHz - 200GHz)	
incumbant spectrum users	DoD Radar, EESS downlinks, radio-astronomy, legacy broadband	EESS passive radiometers	
network availability	~ 99.9%	>= ~99.6 (estimated)	
outage windows	~ minutes-hours. Fewer, longer windows.	~ msec - seconds. Frequent, shorter windows.	
outage dynamics	intermittent and "scheduled"	"scheduled"	
architecture	SAS	SAS (proposed)	
security concerns	high, accomodated by SAS	high, accomodated by SAS	

Table 3 – Comparison of CBRS and RGSS

There are striking similarities between the RGSS proposal and the CBRS deployments (Table 3). Both systems prevent interference by controlling base station Tx power levels and traffic (connected endpoints) based on RF modeling based and a schedule of when incumbent spectrum users will be interfered with. Both systems provide similar levels of network availability, although CBRS windows tend to be fewer and

 $^{^{7}}$ In the U.S., the FCC has the legal authority to allow alternative methods to mitigate interference.

longer, while RGSS windows are considerably shorter and more frequent. Furthermore, both systems use schedule data (in the case of RGSS, the traversal of a given satellite/radiometer, and in CBRS' case, the proximity of radars) to prevent interference.

CBRS provides internal mechanisms to protect sensitive data (e.g., "where Navy ships will be at specific times"). The successful deployment of CBRS indicates that cooperation between government agencies and wireless carriers with similar security concerns (e.g., the location and characteristics of outside plant network elements) is also possible.

It is also interesting that RGSS is compatible with the Wireless Innovation Forum's SAS architecture (Figure 5). In the case of CBRS, the Incoming Incumbent provides schedule (calendar) data to the SAS of when and in which DPAs incumbent spectrum users will be present. In the case of RGSS, the Incoming Incumbent data would be radiometer/satellite traversal data. For RGSS, network infrastructure data could be read from the FCC or directly from carrier databases; similarly, output control information from RGSS would be provided to base stations through the carrier's NMS system.

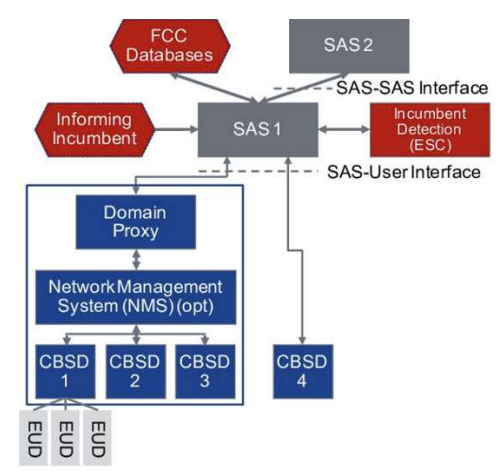


Figure 5 – Spectrum Access System architecture [24]

VII. SUMMARY

In summary, a proof-of-concept Real-Time Geospatial Spectrum Sharing (RGSS) system implementing a simple interference algorithm has a network availability of 99.6% against all operational satellite/radiometers operating at 23.8 GHz. A more sophisticated algorithm that modifies transmission power levels and (if necessary) network traffic can reduce interference to prevent adverse impacts on network availability.

As a software solution, RGSS provides advantages to both the wireless and weather/climate communities. RGSS:

 Enables carriers to optimize network performance by geography, rather than requiring vendors to deliver base stations (gNBs) and user equipment (UEs) designed for worst-case interference scenarios. This is particularly useful in suburban and rural deployments.

- Enables a single software system (with multiple instances to ensure high availability) to support spectrum sharing across multiple mm-wave and sub-mm-wave bands (e.g., 24,52,90, and 130 GHz).
- Easily supports changes to 5G/6G network architecture as well as new network elements or devices.
- Accommodates future radiometer sensors and satellites, and future changes to international standards for isolation between communication networks and radiometer measurements, and
- Provides a simple mechanism to test and police compliance compared with in-situ over the air Total Radiated Power (TRP) measurements.
- Can re-use accepted standards for Spectrum Management Systems, leverage operational experience (including government-industry cooperation) from existing spectrum sharing deployments.

ACKNOWLEDGMENTS

The author is grateful to colleagues from Verizon and Ericsson for their expertise and guidance in 5G 3GPP specifications, architectures, and Open Radio Access Networks. The author is also grateful to colleagues from NOAA, JPL, and The Aerospace Company for their expertise and guidance in radiometry, data extraction from radiometry measurements, and access to raw radiometry data. Finally, the author is grateful to Mathworks for help in modeling 5G waveforms, MIMO transmitter far fields, and access to software modules that support these features.

REFERENCES

- Kyung Mum, "CBRS: New shared spectrum enables flexible indoor and outdoor mobile solutions and new business models", CBRS Alliance, https://ongoalliance.org/wp-content/uploads/2018/05/Mobile-Experts-CBRS-Overview-FINAL.pdf
- [2] Elliot Eichen, "Real-Time Geographical Spectrum Sharing by 5G Networks and Earth Exploration Satellite Services," 2019 IEEE International Symposium on Dynamic Spectrum Access Networks (DySPAN), 2019, doi: 10.1109/DySPAN.2019.8935715
- [3] A. Witze, "5G Data Networks Threaten Forecasts: Wireless Technology Could Interfere with Earth Observations," *Nature*, vol. 569, no. 17
- [4] G. Popkin, "Forecasters fear 5G wireless technology will muck up weather predictions" Science pp 528-529 (Aug 2019).
- [5] Dual Active Protocol Stack (DAPS) handover. 3GPP TS 38.300 version 16.2.0 Rel 16, 9.0 – Mobility and State Transitions
- [6] "Modelling and simulation of IMT networks and systems for use in sharing and compatibility studies", Recommendation ITU-R M.2101-0 (02/2017)
- [7] Results from NASA/NOAA Sharing Studies on WRC-19 Agenda Item1.13,https://science.house.gov/imo/media/doc/Study%20prepared% 20by%20NOAA%20and%20NASA%20-%20Results%20from%20NASANOAA%20Sharing%20Studies%20on %20WRC-19%20Agenda%20Item%201.13.pdf
- [8] Hu, X., Fan, H., Cai, M., Sejas, S. A., Taylor, P., & Yang, S. (2020). A less cloudy picture of the inter-model spread in future global warming projections. *Nature Communications*, 11(1), 1–11. https://doi.org/ 10.1038/s41467-020-18227-9
- [9] Yousefvand, M., Wu, C.-T. M., Wang, R.-Q., Brodie, J., & Mandayam, N. (2020). Modeling the Impact of 5G Leakage on Weather Prediction, https://arxiv.org/abs/2008.13498

- [10] "Typical technical and operational characteristics of Earth explorationsatellite service (passive) systems using allocations between 1.4 and 275 GHz", Recommendation ITU-R RS.1861 (01/2010)
- [11] Brandon, Rhodes, "Skyfield: High precision research-grade positions for planets and Earth satellites generator", https://ui.adsabs.harvard.edu/abs/2019ascl.soft07024R
- [12] Source of TLE data: https://celestrak.com/
- [13] WMO Observing Systems Capability Analysis and Review Tool (OSCAR) https://space.oscar.wmo.int/
- [14] Mitnik, L. M., Kuleshov, V. P., Mitnik, M. L., Streltsov, A. M., Chernyavsky, G. M., & Cherny, I. V. (2017). Microwave Scanner-Sounder MTVZA-GY on New Russian Meteorological Satellite Meteor-M No. 2: Modeling, Calibration, and Measurements. *IEEE Journal of Selected Topics in Applied Earth Observations and Remote Sensing*, 10(7), 3036–3045. https://doi.org/10.1109/JSTARS.2017.2695224
- [15] Gaiser, P. ., St Germain, K. ., Twarog, E. ., Poe, G. ., Purdy, W., Richardson, D., Chang, P. (2004). The WindSat spaceborne polarimetric microwave radiometer: sensor description and early orbit performance. *IEEE Transactions on Geoscience and Remote Sensing*, 42(11), 2347– 2361. https://doi.org/10.1109/TGRS.2004.836867
- [16] Draper, D. W., Newell, D. A., Wentz, F. J., Krimchansky, S., & Skofronick-Jackson, G. M. (2015). The Global Precipitation Measurement (GPM) Microwave Imager (GMI): Instrument Overview and Early On-Orbit Performance. *IEEE Journal of Selected Topics in*

- Applied Earth Observations and Remote Sensing, 8(7), 3452–3462. https://doi.org/10.1109/JSTARS.2015.2403303
- [17] https://sounder.gesdisc.eosdis.nasa.gov/opendap/JPSS1_Sounder_ Level1//SNDRJ1ATMSL1B.2/2021/contents.html
- [18] Pivot 5G 28GHz Network Repeater Data Sheet, https://pivotalcommware.com/pivot-5g/
- [19] Qualcom ATM547 mmWave Antenna Module, https://www.qualcomm.com/products/qtm547-mmwave-antenna-module, and https://www.qualcomm.com/media/documents/files/qtm547-mmwave-antenna-module-product-brief.pdf
- [20] FCC ET Docket No. 21-186, Qualcom Inc., https://ecfsapi.fcc.gov/file/10628521702445/06-28-2021%20Qualcomm%2024%20GHz%20Unwanted%20Emissions.pdf
- [21] Weng, Fuzhong, Yang, Hu, "Validation of ATMS Calibration Accuracy Using Suomi NPP Pitch Maneuver Observations", Remote Sensing pp2072-4292 (2016) doi:10.3390/rs8040332
- [22] Universal Mobile Telecommunications System (UMTS); Physical layer procedures (FDD), 3GPP TS 25.214 Section 1.5 "Uplink Power Control". Also, ref [7] to see how this impacts UE contributions to OOB emissions.
- [23] Wireless Innovation Forum, CBRS Incumbent Protections and Encumbrances Overview, Document WINNF-TR-5003, https://winnf.memberclicks.net/assets/CBRS/WINNF-TR-5003.pd
- [24] Private communication, Wireless Innovation Forum